AN IMPROVED FREQUENCY ESTIMATOR FOR AN ADAPTIVE ACTIVE NOISE CONTROL SCHEME

Michał Meller and Maciej Niedźwiecki

Faculty of Electronics, Telecommunications and Computer Science, Department of Automatic Control
Gdańsk University of Technology, ul. Narutowicza 11/12, 80-233, Gdańsk, Poland
phone: +48 58 3472519; fax: +48 58 3415821, e-mails: michal.meller@eti.pg.gda.pl, maciekn@eti.pg.gda.pl.
web: www.eti.pg.gda.pl

ABSTRACT

An improved frequency tracker is proposed for the recently introduced self optimizing narrowband interference canceller (SONIC). The scheme is designed for disturbances with quasi-linear frequency modulation and, under second-order Gaussian random-walk assumption, can be shown to be statistically efficient. One real-world experiment and several simulations show that a considerable improvement in disturbance rejection may be achieved with the new algorithm.

1. INTRODUCTION

Consider the problem of cancellation of a nonstationary narrowband disturbance $d(t)$ acting at the output of unknown complex-valued linear stable single-input single-output system governed by

$$y(t) = K_{\rm p}(q^{-1})u(t-1) + d(t) + v(t) \tag{1}$$

where $t = \ldots,-1,0,1,\ldots$ denotes discrete time, q^{-1} is the backward-shift operator $q^{-1}u(t) = u(t-1)$, $y(t)$ is the system output, $u(t)$ is the cancellation signal, $v(t)$ is a wideband noise and $K_{\rm p}(q^{-}1)$ is the transfer function of a stable linear plant (often called secondary path), $K_{\rm p}(q^{-1}) = \sum_{n=0}^{\infty} h(n)q^{-n}$, $\sum_{n=0}^{\infty}|h(n)| < \infty$, $K_{\rm p}(e^{-j\omega}) \neq 0, \forall \omega \in [-\pi,\pi)$.

Since elimination of harmonic disturbances may be important to maintain process quality, the problem was solved by many authors, under different assumptions and using different approaches. For instance, when a reference sensor can be placed close to the source of the disturbance, an adaptive feedforward controller based on a variant of filtered-x least mean squares (FX-LMS) algorithm is usually the solution of choice [1]. When such a signal is not available, the problem is more difficult. Then, one of the most common solutions is based on the combination of the FX-LMS algorithm with the internal model control (IMC) architecture. Other successful approaches are based on the internal model principle [2] or phase-locked loops [3] – for a more complete overview of the existing approaches see e.g. [4].

A new approach, based on coefficient fixing and adaptive gain scheduling, has been introduced recently [5], [6]. Unlike numerous previous attempts, it requires little or no prior knowledge of the plant. Furthermore, due to parsimonious controller parameterization, introduction of additional excitation into the loop is not necessary, even when the plant varies over time.

The simplified version of the xSONIC (extended self-optimizing narrowband interference canceller) control algorithm, presented in [6], consists of two loops. The inner loop, which computes the cancellation signal, takes the form

$$\begin{aligned}
\widehat{d}(t+1|t) &= e^{j\widehat{\omega}(t|t-1)}[\widehat{d}(t|t-1) + \widehat{\mu}(t)y(t)] \\
\widehat{\omega}(t+1|t) &= \Omega[\mathscr{Y}(t)] \\
u(t) &= -\frac{\widehat{d}(t+1|t)}{k_{\rm n}}\,,
\end{aligned} \tag{2}$$

where $\widehat{d}(t+1|t)$ is the one-step-ahead prediction of the disturbance, $\widehat{\omega}(t+1|t)$ is the one-step-ahead prediction (based on the available observation history $\mathscr{Y}(t) = \{y(i), i \leq t\}$) of the unknown and possibly time-varying instantaneous frequency of the disturbance $\omega(t)$, and $k_{\rm n}$ is the nominal (assumed) gain of the plant at the frequency $\widehat{\omega}(t|t-1)$, usually different from the true plant's gain $K_{\rm p}(e^{-j\widehat{\omega}(t|t-1)})$ (prior knowledge of the plant improves cancellation results; when no such information is available, one may simply set $k_{\rm n} = 1$, see [6]). Finally $\widehat{\mu}(t)$ is a *complex-valued* adaptation gain. Inclusion of a complex gain is an important feature of the proposed approach, as it allows one to counterbalance *any* discrepancy between the plant and its nominal model.

The second, outer loop, adjusts $\widehat{\mu}(t)$ so as to: 1. Compensate differences between the plant and the assumed nominal gain. 2. Match the closed loop's bandwidth to the rate of nonstationarity of the system. It takes the form

$$\begin{aligned}
z(t) &= e^{j\widehat{\omega}(t|t-1)}\big[(1-c_\mu)z(t-1) - \frac{c_\mu}{\widehat{\mu}(t)}y(t-1)\big] \\
r(t) &= \rho r(t) + |z(t)|^2 \\
\widehat{\mu}(t) &= \widehat{\mu}(t-1) - \frac{y(t)z^*(t)}{r(t)}
\end{aligned} \tag{3}$$

where $c_\mu > 0$ is a small positive constant and $\rho \cong 1$, $0 < \rho < 1$, is the forgetting constant which decides upon the effective adjustment memory length.

The version of xSONIC presented in [6] was fitted with a general-purpose frequency tracker

$$\begin{aligned}
\widehat{\omega}(t+1|t) &= \widehat{\omega}(t|t-1) + \eta g(t) \\
g(t) &= {\rm Arg}\left[\frac{\widehat{d}(t+1|t)}{\widehat{d}(t|t-1)e^{j\widehat{\omega}(t|t-1)}}\right]
\end{aligned} \tag{4}$$

where ${\rm Arg}[\cdot]$ denotes principal argument of a complex number and $\eta > 0$ denotes a small adaptation gain.

This work was supported by the Foundation for the Polish Science, the National Centre for Research and Development and by the European Union from the European Social Fund under the Human Capital Operational Programme and the Innodoktorant project

 ISSN 2076-1465

This paper introduces an improved frequency tracker for the xSONIC controller and presents its analysis. The original scheme (4) is extended by inclusion of estimation of local frequency rate. The reason for such an upgrade is the fact that frequency of many real-world disturbances varies in an approximately piecewise-linear manner [7]. Exploiting this feature leads to more accurate tracking of frequency which, in turn, improves the quality of disturbance rejection.

The analysis of the proposed tracker shows that, for Gaussian random-walk frequency rate changes, it is a statistically efficient estimation procedure. Furthermore, numerous simulation experiments confirm that the resulting xSONIC controller is robust to modeling errors, i.e., it performs well even if the underlying assumptions are not fulfilled.

2. THE PROPOSED ALGORITHM

2.1 Improved frequency estimator

The proposed frequency tracking scheme takes the form

$$\begin{aligned}\widehat{\alpha}(t+1|t) &= \widehat{\alpha}(t|t-1)+\eta_\alpha g(t)\\ \widehat{\omega}(t+1|t) &= \widehat{\omega}(t|t-1)+\widehat{\alpha}(t+1|t)+\eta_\omega g(t)\\ g(t) &= \mathrm{Arg}\left[\frac{\widehat{d}(t+1|t)}{\widehat{d}(t|t-1)e^{j\widehat{\omega}(t|t-1)}}\right]\end{aligned} \tag{5}$$

where $\widehat{\alpha}(t+1|t)$ is the one-step-ahead prediction of the frequency rate $\alpha(t)=\omega(t)-\omega(t-1)$, while η_α and η_ω are small gains satisfying the condition $0<\eta_\alpha\ll\eta_\omega$. Note that for $\eta_\alpha=0$ and under zero initial conditions, (5) reduces to (4).

Compared to e.g. the state-of-the art multiple linear frequency tracker (MFT-L) [8], the proposed algorithm is very simple. Rather unexpectedly, this tracker outperforms MFT-L in many aspects. The analysis of MFT-L, performed in [8], showed that it nearly reaches the so-called posterior Cramér-Rao bounds (PCRB) [9], which hold for frequency and frequency rate tracking and limit the efficiency of any tracking scheme (the classical Cramér-Rao bound does not apply to systems with random parameters). The loss in performance, ranged from 1% to 7% for frequency tracking and from 9% to 28% for frequency rate tracking. Moreover, the optimal settings for MFT-L were found to depend on the tracking objective (frequency or frequency rate). We will show that the algorithm (5) is able to reach both bounds, and that it reaches them simultaneously.

2.2 Analysis of the Algorithm

To avoid unnecessary complications, our discussion will be carried for the constant-amplitude ($|d(t)|=a_0$) disturbance model

$$\begin{aligned}d(t+1) &= e^{j\omega(t)}d(t)\\ \omega(t+1) &= \omega(t)+\alpha(t+1)\\ \alpha(t+1) &= \alpha(t)+w_\alpha(t+1)\,,\end{aligned} \tag{6}$$

where $\omega(t)$ and $\alpha(t)$ denote the local frequency and frequency rate (trend), respectively, and $w_\alpha(t)$ is the one-step change of frequency rate. Furthermore, we will assume that $v(t)$ is a zero-mean complex Gaussian circular white noise with variance σ_v^2, and that $w_\alpha(t)$, independent of $v(t)$, is a zero-mean Gaussian white noise with variance σ_α^2.

The latter assumption means that frequency obeys a second-order random walk model

$$(1-q^{-1})^2\omega(t)=w_\alpha(t) \tag{7}$$

which can be considered a stochastic extension of a linear frequency modulation scheme[1], where

$$\omega(t)=\omega_0+\Delta_\omega t\,. \tag{8}$$

In a short time frame both models yield similar frequency trajectories. The advantage of the stochastic approach over the much simpler deterministic case stems from the fact that it incorporates modeling noise. This makes the stochastic model more "realistic".

It is clear that, in order to reject disturbance (6), one should generate such a narrowband signal $u(t)$ which – after passing through the plant – will destructively interfere with $d(t)$. Suppose that the frequency varies sufficiently slowly. The output of the plant $K_\mathrm{p}(q^{-1})$, excited by $u(t)$, can then be approximated using a simple scale-and-shift model

$$K_\mathrm{p}(q^{-1})u(t-1)\cong k_\mathrm{p}u(t-1) \tag{9}$$

where $k_\mathrm{p}=\frac{1}{T}\sum_{n=t-T+1}^{t}K_\mathrm{p}(e^{-j\widehat{\omega}(t|t-1)})$ is the average frequency response of the plant in the local analysis window $[t-T+1,t]$ of width T.

Using (2) and (9), the system equation (1) can be rewritten as

$$y(t)\cong d(t)-\frac{k_\mathrm{p}}{k_\mathrm{n}}\,\widehat{d}(t|t-1)+v(t)=c(t)+v(t) \tag{10}$$

where $c(t)=d(t)-\frac{k_\mathrm{p}}{k_\mathrm{n}}\,\widehat{d}(t|t-1)$ denotes the cancellation error. The quantity $\beta=k_\mathrm{p}/k_\mathrm{n}$, further referred to as modeling error, will be assumed constant.

Let $\Delta\widehat{\omega}(t)=\omega(t)-\widehat{\omega}(t|t-1)$ and $\Delta\widehat{\alpha}(t)=\alpha(t)-\widehat{\alpha}(t|t-1)$ denote the frequency tracking error and the frequency rate tracking error, respectively. Additionally, let $x(t)=c(t)d^*(t)$ and $z(t)=v(t)d^*(t)$. Note that $z(t)$ is a zero-mean circular white Gaussian noise with variance $\sigma_v^2a_0^2$. Using the approximating linear filter (ALF) method, introduced in [10] for the purpose of analysis of adaptive notch filters, one can arrive at the following approximations

$$\begin{aligned}x(t+1) &= (1-\mu\beta)x(t)-\mu\beta z(t)+ja_0^2\Delta\widehat{\omega}(t)\\ \Delta\widehat{\alpha}(t+1) &= \Delta\widehat{\alpha}(t)+w_\alpha(t+1)-\eta_\alpha\mathrm{Im}\left\{\frac{\mu\beta}{a_0^2}\big[x(t)+z(t)\big]\right\}\\ \Delta\widehat{\omega}(t+1) &= \Delta\widehat{\omega}(t)+\Delta\widehat{\alpha}(t+1)\\ &\quad-\eta_\omega\mathrm{Im}\left\{\frac{\mu\beta}{a_0^2}\big[x(t)+z(t)\big]\right\}.\end{aligned} \tag{11}$$

3. TRACKING AND CANCELLATION CAPABILITIES

Observe that any occurrence of β in (11) is always accompanied by μ. Therefore, no matter what modeling error is, its influence can be always 'undone' with the proper choice of

[1] Note that linear modulation (8) is governed by $(1-q^{-1})^2\omega(t)=0$, which means that (7) can be regarded as a "perturbed" linear model, and the resulting frequency modulation – as "quasi-linear".

the complex-valued gain μ. In [5] we show that such a compensation actually takes place when the adjustment algorithm (3) is used. Keeping this in mind, in the remaining part of our analysis we will assume, without any loss of generality, that $\beta = 1$.

Let $x_{\mathrm{R}}(t) = \mathrm{Re}[x(t)]$, $x_{\mathrm{I}}(t) = \mathrm{Im}[x(t)]$, $z_{\mathrm{R}}(t) = \mathrm{Re}[z(t)]$, and $z_{\mathrm{I}}(t) = \mathrm{Im}[z(t)]$. Note that $z_{\mathrm{R}}(t)$ and $z_{\mathrm{I}}(t)$ are independent zero-mean Gaussian white noises with identical variances equal to $\sigma_v^2 a_0^2/2$. Solving equations (11) with respect to $x_{\mathrm{R}}(t)$, $x_{\mathrm{I}}(t)$, $\Delta\widehat{\omega}(t)$, and $\Delta\widehat{\alpha}(t)$, one obtains

$$\begin{aligned} x_{\mathrm{R}}(t) &= F(q^{-1})z_{\mathrm{R}}(t) \\ x_{\mathrm{I}}(t) &= G_1(q^{-1})z_{\mathrm{I}}(t) + G_2(q^{-1})w_\alpha(t) \\ \Delta\widehat{\omega}(t) &= H_1(q^{-1})z_{\mathrm{I}}(t) + H_2(q^{-1})w_\alpha(t) \\ \Delta\widehat{\alpha}(t) &= I_1(q^{-1})z_{\mathrm{I}}(t) + I_2(q^{-1})w_\alpha(t) \end{aligned} \tag{12}$$

where

$$\begin{aligned} F(q^{-1}) &= -\frac{\mu q^{-1}}{1-(1-\mu)q^{-1}} \\ G_1(q^{-1}) &= -a_0^2\mu\big[q^{-1} + (\eta_\alpha + \eta_\omega - 2)q^{-2} \\ &\qquad + (1-\eta_\omega)q^{-3}\big]/D(q^{-1}) \\ G_2(q^{-1}) &= -a^4 q^{-1}/D(q^{-1}) \\ H_1(q^{-1}) &= -\mu q^{-1}(1-q^{-1})\big[(\eta_\alpha + \eta_\omega) - \eta_\omega q^{-1}\big]/D(q^{-1}) \\ H_2(q^{-1}) &= a_0^2\big[1-(1-\mu)q^{-1}\big]/D(q^{-1}) \\ I_1(q^{-1}) &= -\mu\eta_\alpha q^{-1}(1-q^{-1})^2/D(q^{-1}) \\ I_2(q^{-1}) &= a_0^2\big[1 + (\mu-2)q^{-1} \\ &\qquad + (1-\mu+\eta_\omega\mu)q^{-2}\big]/D(q^{-1}) \end{aligned}$$

and

$$\begin{aligned} D(q^{-1}) = a_0^2\Big\{ & 1 + (-3+\mu)q^{-1} \\ & + \big[3 + \mu(-2 + \eta_\alpha + \eta_\omega)\big]q^{-2} \\ & + (-1 + \mu - \eta_\omega\mu)q^{-3}\Big\} \end{aligned} \tag{13}$$

3.1 Frequency Tracking

Using basic facts from the linear filtering theory [11], one can evaluate the steady-state mean-squared values of frequency and frequency rate tracking errors:

$$\begin{aligned} \mathrm{E}[|\Delta\widehat{\omega}(t)|^2] &= J[H_1(z^{-1})]\mathrm{E}[z_{\mathrm{I}}^2(t)] + J[H_2(z^{-1})]\mathrm{E}[w_\alpha^2(t)] \\ \mathrm{E}[|\Delta\widehat{\alpha}(t)|^2] &= J[I_1(z^{-1})]\mathrm{E}[z_{\mathrm{I}}^2(t)] + J[I_2(z^{-1})]\mathrm{E}[w_\alpha^2(t)] \end{aligned} \tag{14}$$

where

$$J[X(z^{-1})] = \frac{1}{2\pi j}\oint X(z)X(z^{-1})\frac{dz}{z}$$

is the integral evaluated along unit circle and $X(z^{-1})$ is a stable proper rational transfer function.

Symbolic expressions relating mean-squared errors $\mathrm{E}[|\Delta\widehat{\omega}(t)|^2]$ and $\mathrm{E}[|\Delta\widehat{\alpha}(t)|^2]$ to the values of parameters μ, η_ω and η_α, disturbance amplitude a_0^2 and variance σ_α^2 are very long and therefore they will not be shown here. Our further discussion is based on the results obtained using MATLAB Symbolic Toolbox and on numerical methods.

σ_α^2	μ	η_ω	η_α	$\mathrm{E}[\lvert\Delta\widehat{\omega}(t)\rvert^2]$	Simulation	PCRB
10^{-8}	0.104	0.050	0.0013	$2.27\cdot10^{-4}$	$2.30\cdot10^{-4}$	$2.27\cdot10^{-4}$
10^{-7}	0.153	0.072	0.0027	$7.43\cdot10^{-4}$	$7.65\cdot10^{-4}$	$7.43\cdot10^{-4}$
10^{-6}	0.224	0.103	0.0056	$2.46\cdot10^{-4}$	$2.66\cdot10^{-4}$	$2.46\cdot10^{-4}$

(a) SNR=0dB

σ_α^2	μ	η_ω	η_α	$\mathrm{E}[\lvert\Delta\widehat{\omega}(t)\rvert^2]$	Simulation	PCRB
10^{-8}	0.153	0.072	0.0027	$7.43\cdot10^{-5}$	$7.44\cdot10^{-5}$	$7.43\cdot10^{-5}$
10^{-7}	0.224	0.103	0.0056	$2.46\cdot10^{-4}$	$2.48\cdot10^{-4}$	$2.46\cdot10^{-4}$
10^{-6}	0.329	0.146	0.0115	$8.36\cdot10^{-4}$	$8.39\cdot10^{-4}$	$8.36\cdot10^{-4}$

(b) SNR=10dB

σ_α^2	μ	η_ω	η_α	$\mathrm{E}[\lvert\Delta\widehat{\omega}(t)\rvert^2]$	Simulation	PCRB
10^{-8}	0.224	0.103	0.0056	$2.46\cdot10^{-5}$	$2.47\cdot10^{-5}$	$2.46\cdot10^{-5}$
10^{-7}	0.329	0.146	0.0115	$8.36\cdot10^{-5}$	$8.37\cdot10^{-5}$	$8.36\cdot10^{-5}$
10^{-6}	0.482	0.203	0.0230	$2.93\cdot10^{-4}$	$2.93\cdot10^{-4}$	$2.93\cdot10^{-4}$

(c) SNR=20dB

Table 1: Optimal settings for a tracking of frequency. Comparison of predicted mean-squared error, simulation results and PCRB.

Table I shows the values of the parameters μ, η_ω and η_α which minimize frequency tracking error for SNR $= 10\log(a_0^2/\sigma_v^2) \in \{0\mathrm{dB}, 10\mathrm{dB}, 20\mathrm{dB}\}$ (low, medium, and high SNR) and $\sigma_w^2 \in \{10^{-8},\ 10^{-7},\ 10^{-6}\}$. The settings were found using exhaustive numerical search. Additionally, Table I presents theoretical predictions of mean-squared estimation errors (obtained by the ALF method), their actual values (obtained using simulations) and corresponding PCRB's. The simulation results were obtained by combined ensemble averaging (50 realizations of $\{v(t),\ w(t)\}$) and time averaging ($t \in [20001, 100000]$). To ensure that steady-state was reached, the results obtained for the first 20000 time steps were discarded. The proposed algorithm was used with the static plant $K_{\mathrm{p}}(q^{-1}) = 1$. The nominal plant gain was set equal to the true gain $k_{\mathrm{n}} = k_{\mathrm{p}} = 1$.

Table II shows similar results obtained for frequency rate optimization.

The results gathered in Tables I and II are quite remarkable. Not only is the proposed algorithm able to reach both PCRB's, but it also attains them for the very same parameter settings. Simulations confirm almost-statistical efficiency of (5). Minor discrepancies, none of which exceeds 0.5%, occur mostly for low SNR's and large σ_α and may be attributed to the phenomenon of large deviations (not covered by ALF method).

3.2 Cancellation

The fact that the proposed frequency estimator can be made statistically efficient is undoubtedly its strong point. However, our main interest lies in maximizing its disturbance rejection capability, i.e. in minimizing $\mathrm{E}[|c(t)|^2]$. This can also be evaluated using ALF equations. Note that $\mathrm{E}[|x(t)|^2] = a_0^2\mathrm{E}[|c(t)|^2]$. Since $w(t)$, $z_{\mathrm{R}}(t)$ and $z_{\mathrm{I}}(t)$ are independent, it holds that

$$\begin{aligned} \mathrm{E}[|x(t)|^2] = {} & J[F(z^{-1})]\mathrm{E}[z_{\mathrm{R}}^2(t)] + J[G_1(z^{-1})]\mathrm{E}[z_{\mathrm{I}}^2(t)] \\ & + J[G_2(z^{-1})]\mathrm{E}[w_\alpha^2(t)]\ . \end{aligned} \tag{15}$$

σ_α^2	μ	η_ω	η_α	$\mathrm{E}[\lvert\Delta\widehat{\alpha}(t)\rvert^2]$	Simulation	PCRB
10^{-8}	0.104	0.050	0.0013	$3.89\cdot10^{-7}$	$3.89\cdot10^{-7}$	$3.89\cdot10^{-7}$
10^{-7}	0.153	0.072	0.0027	$2.67\cdot10^{-6}$	$2.69\cdot10^{-6}$	$2.67\cdot10^{-6}$
10^{-6}	0.224	0.103	0.0056	$1.83\cdot10^{-5}$	$1.87\cdot10^{-5}$	$1.83\cdot10^{-5}$

(a) SNR=0dB

σ_α^2	μ	η_ω	η_α	$\mathrm{E}[\lvert\Delta\widehat{\alpha}(t)\rvert^2]$	Simulation	PCRB
10^{-8}	0.153	0.072	0.0027	$2.67\cdot10^{-7}$	$2.67\cdot10^{-7}$	$2.67\cdot10^{-7}$
10^{-7}	0.224	0.103	0.0056	$1.83\cdot10^{-6}$	$1.84\cdot10^{-6}$	$1.83\cdot10^{-6}$
10^{-6}	0.329	0.146	0.0115	$1.27\cdot10^{-5}$	$1.27\cdot10^{-5}$	$1.27\cdot10^{-5}$

(b) SNR=10dB

σ_α^2	μ	η_ω	η_α	$\mathrm{E}[\lvert\Delta\widehat{\alpha}(t)\rvert^2]$	Simulation	PCRB
10^{-8}	0.224	0.103	0.0056	$1.83\cdot10^{-7}$	$1.84\cdot10^{-7}$	$1.83\cdot10^{-7}$
10^{-7}	0.329	0.146	0.0115	$1.27\cdot10^{-6}$	$1.27\cdot10^{-6}$	$1.27\cdot10^{-6}$
10^{-6}	0.482	0.203	0.0230	$8.83\cdot10^{-6}$	$8.83\cdot10^{-6}$	$8.83\cdot10^{-6}$

(c) SNR=20dB

Table 2: Optimal settings for a tracking of frequency rate. Comparison of predicted mean-squared error, simulation results and PCRB.

σ_w^2	μ	η_ω	η_α	$\mathrm{E}[\lvert c(t)\rvert^2]$	Simulation
10^{-9}	0.076	0.068	0.0013	$7.79\cdot10^{-3}$	$7.79\cdot10^{-3}$
10^{-8}	0.113	0.096	0.0026	$1.17\cdot10^{-2}$	$1.17\cdot10^{-2}$
10^{-7}	0.169	0.133	0.0054	$1.79\cdot10^{-2}$	$1.79\cdot10^{-2}$
10^{-6}	0.253	0.183	0.0110	$2.76\cdot10^{-2}$	$2.77\cdot10^{-2}$

Table 3: Optimal cancellation settings. Comparison of predicted mean-squared cancellation error and simulation results. SNR=10 dB, $a_0^2=1$.

Again, due to excessive complexity, the symbolic expression for $\mathrm{E}[\lvert x(t)\rvert^2]$ will not be provided here.

Table III shows the values of μ, η_ω, η_α which minimize the mean-squared cancellation error for $a_0^2=1$, SNR $=10\log(a_0^2/\sigma_v^2)$ =10 dB and $\sigma_w^2\in\{10^{-9},10^{-8},10^{-7},10^{-6}\}$. Additionally, the table provides ALF-based evaluations of $\mathrm{E}[\lvert c(t)\rvert^2]$, and the actual cancellation results obtained by means of computer simulation.

Observe almost perfect agreement between the ALF-based evaluations and simulation results. Note also, that settings which minimize the mean-squared cancellation error differ from those minimizing the mean-squared frequency and frequency rate tracking errors.

3.3 Self-optimization penalty

So far, we have assumed that the gain μ is constant. To measure performance losses introduced by xSONIC's self-optimization loop (3), all simulations from Section IV-B were repeated with some modifications. To introduce modeling error, the nominal plant's gain was altered to $k_\mathrm{n}=2e^{j\pi/4}$. The parameters η_ω and η_α were set constant according to Table III, while μ was automatically tuned using (3) with $c_\mu=0.02$ and $\rho=0.999$.

The obtained results, summarized in Table IV, show that performance degradation caused by self-optimization is, from a practical viewpoint, very small (less than 0.5 dB in the worst case). For $\sigma_w^2=10^{-6}$ occasional large frequency deviations, causing local error bursts, were observed. Such cases were excluded from averaging.

σ_w^2	Auto-adjustment	
	off	on
10^{-9}	$7.79\cdot10^{-3}$ (-21.1 dB)	$8.06\cdot10^{-3}$ (-20.9 dB)
10^{-8}	$1.17\cdot10^{-2}$ (-19.3 dB)	$1.21\cdot10^{-2}$ (-19.2 dB)
10^{-7}	$1.79\cdot10^{-2}$ (-17.5 dB)	$1.86\cdot10^{-2}$ (-17.3 dB)
10^{-6}	$2.77\cdot10^{-2}$ (-15.6 dB)	$2.93\cdot10^{-2}$ (-15.3 dB)

Table 4: Performance losses caused by self-optimization. SNR=10 dB, $a_0^2=1$.

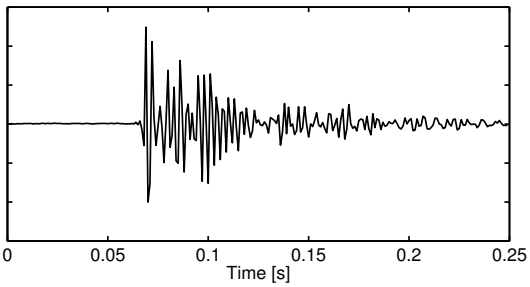

Figure 1: First 250 coefficients of the estimated impulse response of the controlled plant (secondary acoustic path, including transport and processing delays).

3.4 Tuning guidelines

Evaluating roots of the polynomial (13), one can arrive at the following (sufficient) stability conditions: $\mu<1$, $\eta_\omega<1$, $\eta_\alpha<1$ and $\eta_\alpha<\mu\eta_\omega$ which shed some light on the issue of tuning of the algorithm (5). The lower bound $\mu_{\min}$ on μ can be evaluated by observing the steady-state behavior of xSONIC equipped with the older version of frequency tracker, i.e. by setting $\eta_\alpha=0$. Alternatively, the adaptation law in (3) may be modified so as to prevent μ from taking too small values. The gain η_α can then be set as $\eta_\alpha=f\mu_{\min}\eta_\omega$ where f plays a role of "safety factor", e.g. $f=0.1$.

4. REAL-WORLD EXPERIMENT

An acoustic experiment was performed using a standard laptop PC. The disturbance was generated by the left loudspeaker, placed about 1 m away from the microphone. The cancellation signal was generated by the second loudspeaker, located approximately 30 cm away from the microphone (which resulted in a 1 ms propagation delay). The system operated at a sampling rate of 1 kHz.

Fig. 1 shows the first 250 coefficients of the estimated impulse response of the plant (often referred to as the secondary acoustic path). Long transport delay, equal to almost 60 sampling intervals, was caused by the hardware (cheap built-in soundcard) and operating system limitations (buffering effect).

An artificially generated sinusoidal signal with the instantaneous frequency varying sinusoidally between 280 Hz and 300 Hz, over a period of 20 s, was used as a disturbance. Under this scenario the largest frequency rate (defined as a derivative of the instantaneous frequency with respect to time) was equal to 3 Hz/s.

The following settings were used: $c_\mu=0.01$, $\rho=0.999$, $\eta_\omega=0.005$, $\eta_\alpha=0.000005$. The nominal model of plant was $k_\mathrm{n}=1$. Additionally, to reduce the risk of erratic behavior during initial phase the maximum allowable values were adopted for $\lvert\widehat{\mu}(t)\rvert$ and $r(t)$, $\mu_{\max}=0.15$, $r_{\max}=20$ (see [6]

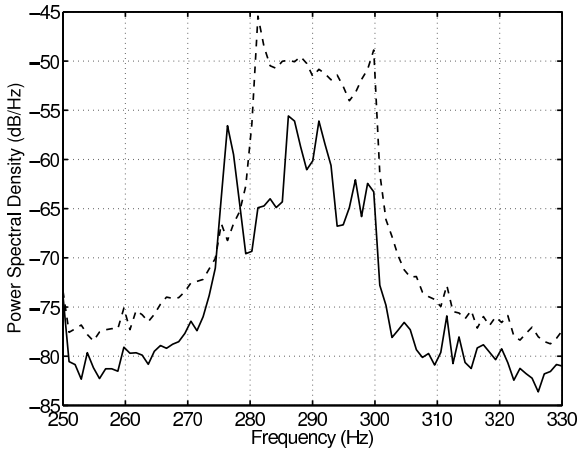

Figure 2: Comparison of power spectral densities of the output signal with (solid line) and without (dashed line) interference cancellation.

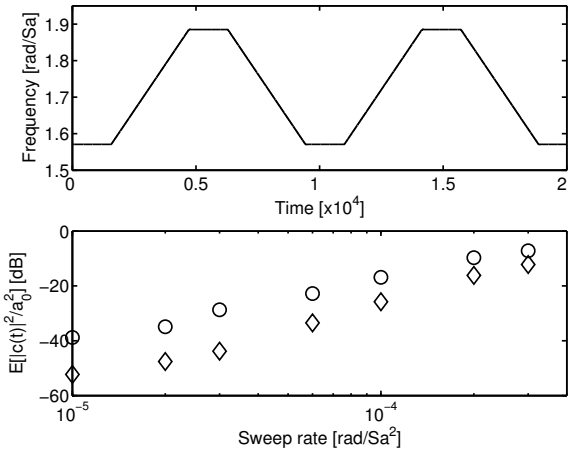

Figure 3: Comparison of xSONIC controllers equipped with two frequency tracking schemes: circles – scheme (4), diamonds – scheme (5). Top figure – fragment of frequency trajectory for $\Delta_\omega = 10^{-4}$. Bottom figure – results.

for a discussion of advisable safety measures and possible extensions).

Fig. 2 shows power spectral densities of the signal recorded by the error microphone with and without disturbance cancellation, averaged over the period of 20s. The obtained degree of improvement varied from 5 dB to 15 dB.

5. SIMULATION RESULTS

An extra set of simulations was arranged to check the improvement which can be obtained by using the scheme (5) in place of (4).

The secondary path was modeled using the impulse response of a real world acoustic plant. The variance of measurement noise $v(t)$ was set to $\sigma_v^2 = 10^{-4}$ and the amplitude of narrowband disturbance $d(t)$ was $a_0 = 1$. The nominal model was equal to the true plant, $k_{\mathrm{n}}(t) = K_{\mathrm{p}}[e^{-j\widehat{\omega}(t+1|t)}]$.

To guarantee fair comparison, the gains η, η_ω and η_α of the compared schemes were tuned optimally using exhaustive numerical search. To reduce number of degrees of freedom a fixed relation $\eta_\alpha = \eta_\omega/100$ was adopted for the proposed scheme. The two remaining parameters, c_μ and ρ, were set to 0.005 and 0.999, respectively. Finally, to improve transients and to reduce the risk of erratic system behavior, the magnitude of $\widehat{\mu}(t)$ was limited to $\mu_{\max} = 0.025$.

Frequency trajectory used in the comparison consisted of 'back-and-forth' linear sweeps [each obeying $\omega(t+1) = \omega(t) \pm \Delta_\omega$, where Δ_ω denotes sweep rate] between $\omega_{\min} = 1.57$ and $\omega_{\max} = 1.88$, separated by shorter constant-frequency periods. The top plot of fig. 3 shows a fragment of a frequency trajectory for a sweep rate equal to 10^{-4}.

The results of the experiment, depicted in the bottom plot of fig. 3, show that a considerable improvement (from 5 to 15 dB) may be expected with the new scheme.

6. CONCLUSIONS

An improved frequency tracker was proposed for the xSONIC canceler. The new algorithm, albeit very simple, is statistically efficient under Gaussian assumptions. Practical effectiveness of the resulting controller was demonstrated with a real-world example and confirmed by simulations.

REFERENCES

[1] S. M. Kuo and D. Morgan, *Active Noise Control Systems: Algorithms and DSP Implementations*. New York: Wiley, 1995.

[2] I. Landau, A. Constantinescu, and D. Rey, "Adaptive narrow band disturbance rejection applied to an active suspension – an internal model principle approach," *Automatica*, vol. 41, pp. 563–574, April 2005.

[3] M. Bodson and S. Douglas, "Adaptive algorithms for the rejection of sinusoidal disturbances with unknown frequency," *Automatica*, vol. 33, pp. 2213–2221, December 1997.

[4] M. Bodson, "Rejection of periodic disturbances of unknown and time-varying frequency," *Int. J. Adapt. Control Signal Process*, vol. 19, pp. 67–88, 2005.

[5] M. Niedźwiecki and M. Meller, "New approach to active noise and vibration control - part 1: the known frequency case," *IEEE Trans. on Signal Processing*, vol. 57, no. 9, pp. 3373–3386, 2009.

[6] ——, "New approach to active noise and vibration control - part 2: the unknown frequency case," *IEEE Trans. on Signal Processing*, vol. 57, no. 9, pp. 3387–3398, 2009.

[7] C. Bohn, A. Cortabarria, V. Härtel, and K. Kowalczyk, "Active control of engine-induced vibrations in automotive vehicles using disturbance observer gain scheduling," *Control Engineering Practice*, vol. 12, pp. 1029–1039, August 2004.

[8] P. Tichavský and P. Händel, "Recursive estimation of frequencies and frequency rates of multiple cisoids in noise," *Signal Processing*, vol. 58, no. 2, pp. 117–129, April 1997.

[9] H. van Trees, *Detection, Estimation and Modulation Theory*. New York: Wiley, 1968.

[10] P. Tichavský and P. Händel, "Two algorithms for adaptive retrieval of slowly time-varying multiple cisoids in noise," *IEEE Trans. on Signal Process.*, vol. 43, pp. 1116—1127, May 1995.

[11] M. Jury, *Theory and Application of the Z-transform Method*. New York: Wiley, 1964.